The Statistical Evaluation of Data Obtained via the Manual Segmentation of MRI Images of a Pathological Tissue

P. Marcon[1], **J. Mikulka**[1], **E. Gescheidtova**[1], **K. Bartusek**[2], **and A. Sprlakova**[3]

[1]FEEC, Department of Theoretical and Experimental Electrical Engineering
Brno University of Technology, Technicka 3082/12, Brno 616 00, Czech Republic
[2]Institute of Scientific Instruments of the ASCR
v.v.i, Kralovopolska 147, Brno 612 64, Czech Republic
[3]Radiological Clinic, The University Hospital Brno
Jihlavska 20, Brno 625 00, Czech Republic

Abstract— The authors present a statistical evaluation of the MRI images of bones and soft tissues. MRI imaging of small bones is a problem issue because the measured bone images are loaded with susceptibility artifacts and low signal-to-noise ratio. Therefore, we compare the commonly used MRI contrast and looking for the best contrast to bone marrow imaging. The acquired images are classified in terms of the signal-to-noise ratio, intensity difference and steepness of the edges.

The aim of this research was to statistically evaluate and determine the deviation of MRI images; this step was performed by several experts. These specialists conducted proper segmenting of pathological and healthy tissues, and they also compared the selected areas. In some cases, especially when the boundaries of the area are not clearly visible, the problem is to delimit the bone marrow area. Therefore, it is not possible to use automatic segmentation algorithms, and we focused on the manual evaluation of the statistical data in the area of the patient's bone marrow pathology (e.g., the probability of cyst formation can be determined from abnormal levels of vitamin D and osteocalcin).

1. INTRODUCTION

The research of pathology of human tissues is currently very interesting [1–4]. Development of the magnetic resonance imaging represent very significant step because this technique provides images with excellent soft tissues contrast [5, 6]. We focus on MRI imaging of small bones, it is a problem issue because the measured bone images are loaded with susceptibility artifacts and low signal-to-noise ratio [7–11].

In our research, we focus on a manual segmentation, data processing and a statistical analysis of MRI data [12]. The main task of our research was to compare the number of MRI contrast and determine the appropriate contrast for an imaging of specific tissues. The second task was statistical data comparison. The method of measurement and data processing was tested on the volunteers with pathology in the area of mandibular bone marrow.

2. STATISTICAL ANALYSIS

For our experiment we have to introduce the notion of a box plot. The box plot (a.k.a. box and whisker diagram) is a standardized way of displaying the distribution of data based on the five number summaries: minimum, first quartile, median, third quartile, and maximum. In the simplest box plot the central rectangle spans the first quartile to the third quartile (the *interquartile range* or *IQR*). A segment inside the rectangle shows the median and "whiskers" above and below the box show the locations of the minimum and maximum [12].

3. EXPERIMENT

In our experiment we used a MR tomograph at the University Hospital Bohunice. The MR tomograph dispose of static field flux density $B_0 = 1.5\,\mathrm{T}$. From the tomograph we obtain images of a mandibular region and of a hip joint region to signal processing. The specialist processed the T_1 Weighted Images without contrast agent — T1W and with Contrast Agent — T1W_ContAgent; T_2 Weighted Images — T2W; Short Tau Inversion Recovery weighted images — STIR and Diffusion Weighted Images — DWI.

The aim of this research was to statistically evaluate and determine the deviation of MRI images; this step was performed by several experts. These ten specialists conducted proper segmenting of pathological and healthy tissues, and they also compared the selected areas. In some cases, especially when the boundaries of the area are not clearly visible, the problem is to delimit the bone marrow area. Therefore, it is not possible to use automatic segmentation algorithms, and we focused on the manual evaluation of the statistical data in the area of the patient's bone marrow pathology (e.g., the probability of cyst formation can be determined from abnormal levels of vitamin D and osteocalcin).

Therefore, the specialists segmenting pathological and healthy tissues, namely: bone and bone marrow; further muscle, fat, ligament, gray matter, white matter, eye. After that they performed a statistical analysis of segmenting area. On the basis of this statistical data from individual human tissues a new statistics (statistic from statistic) was made. By each statistical evaluation of tissue were calculated following statistical quantities: minimum value, maximum value, mean value, standard deviation (S.D.), skewness and kurtosis. The box plots were created.

4. RESULTS

Figure 1 shows two coronal MRI slices of human head. The specialists focus on the segmentation and statistical analysis of mandibular region.

Figure 2 shows also two MR images of human head. Left figure shows a diffusion weighted image of a transversal slice and right figure shows T_2 weighted image of transversal slide. Figure 3 on the left shows T_1 weighted image of the human hip and the right image shows diffusion weighted image of the human hip. As you can see, the diffusion weighted image is affected by artefacts [13, 14].

In Figure 4 you can see the box plot obtained by statistical analysis of bone marrow. This step was performed by several experts. First, these specialists conducted proper segmenting of pathological bone marrow. Second, these specialist made statistical analysis of selected data. We obtain these data from the ten specialists and we made a new statistic. Ideally, the specialists should evaluate the same data, but really as you can see in Figure 4, the data are different. A scattering of obtained data is represent by box plot.

Figure 5 shows a mean values box plot of individual tissues. These data was obteined form

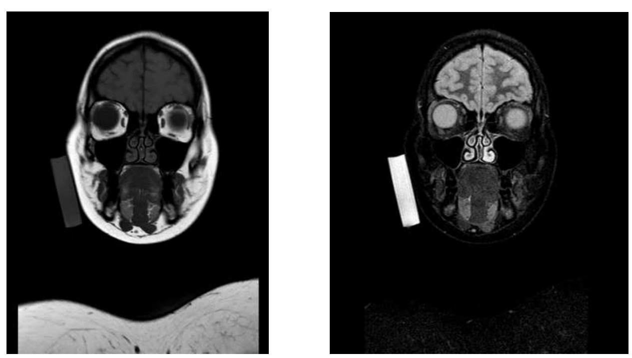

(a) (b)

Figure 1: Coronal slices with 2D imaging of the human head. (a) T1W image. (b) STIR weighted image.

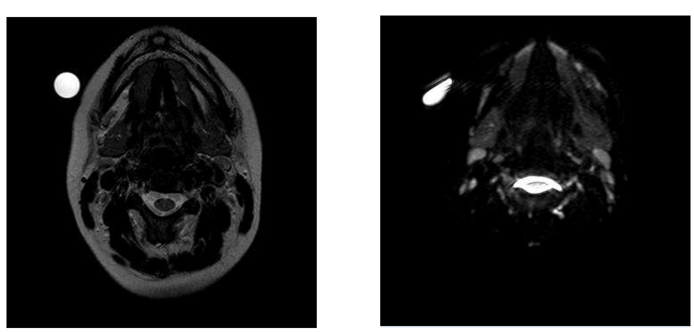

(a) (b)

Figure 2: Transversal slices with 2D imaging of the human head. (a) T2W image. (b) Diffusion weighted image.

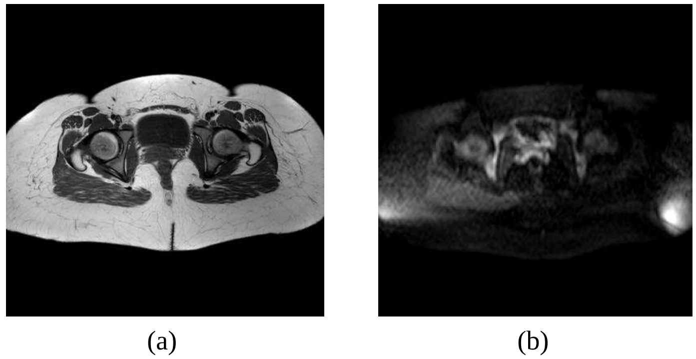

Figure 3: Transversal slices with 2D imaging of the human hip. (a) T1W image. (b) DWI image.

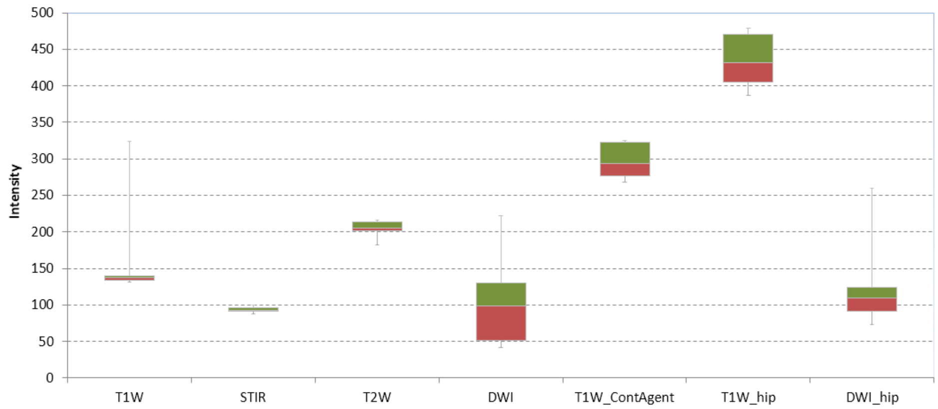

Figure 4: The Box blot obtained by statistical analysis of MR bone marrow data selected and processed by ten specialist.

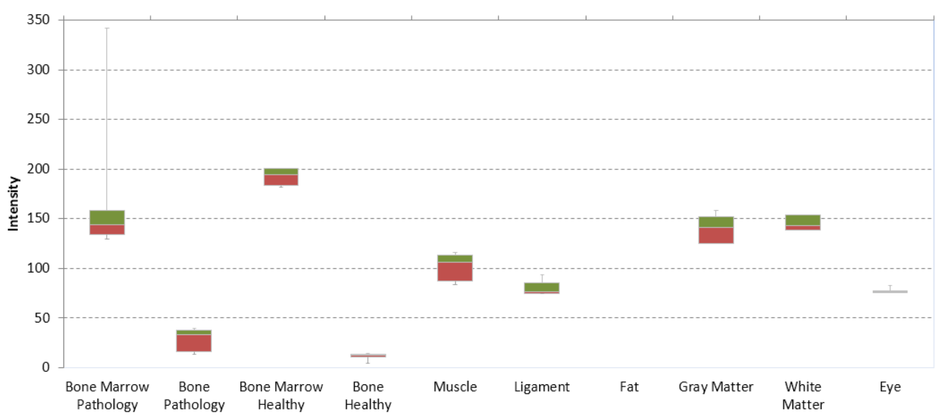

Figure 5: The Box plot of T_1 weighted mean values of individual tissues.

T_1 weighted images of bone marrow, see Figure 1(a). There, the right hand side of mandibula is without bone marrow pathology and left hand side exhibit a bone marrow pathology. The box plot in Figure 5 present differences not only between healthy and pathology bone marrow, but also statistical differences between individual tissues. These data are very useful for programing a automatig segmentation procedure.

5. CONCLUSIONS

We evaluated a statistical analysis of the MR images of bones and soft tissues. Therefore, we compared the commonly used MRI contrast and we found the best contrast to bone marrow imaging, namely T_1 weighted imaging. From the statistical evaluation we created the small database of healthy human tissues: bone, bone marrow, muscle, fat, white matter, gray matter and eye. By each tissue we evaluated following statistical quantities: mean value, standard deviation, skewness and kurtosis. The box plots and small statistic database were created. The results of the statistics data are presented in the Figure 5. This database is used to identification the unknown tissues.

Further, we evaluated the statistical deviation arising by segmentation and determining healthy or pathology human tissues; this step was performed by several experts. These specialists conducted proper segmenting of pathological and healthy tissues, and they also compared the selected areas. First, these specialists conducted proper segmenting of pathological bone marrow. Second, these specialist made statistical analysis of selected data. We obtain data from the ten specialists and we made a new statistic. Ideally, the specialists should evaluate the same data, but really as you can see in Figure 4, the data are different. A scattering of obtained data is represent by box plot.

ACKNOWLEDGMENT

This work was supported in part by the Grant GACR 102/12/1104 and the programme FEKT-S-14-2545 and Education for Competitiveness Operative Programme CZ.1.07.2.3.00.20.0175 (Electro-researcher).

REFERENCES

1. Andris, P. and I. Frollo, "Measurement of magnetic field with background using a low-field NMR scanner," *Measurement Science Technology*, Vol. 23, 2012.
2. Marcon, P., K. Bartusek, and M. Cap, "Multiparametric data collection and data processing of animal tissues in MRI images," *PIERS Proceedings*, 358–362, Moscow, Russia, Aug. 19–23, 2012.
3. Gogola, D., A. Krafcik, O. Strbak, and I. Frollo, "Magnetic resonance imaging of surgical implants made from weak magnetic materials," *Measurement Science Review*, Vol. 13, No. 4, 165–168, 2013.
4. Mikulka, J., E. Gescheidtova, and K. Bartusek, "Processing of MR slices of human liver for volumetry," *PIERS Proceedings*, 202–204, Xi'an, China, Mar. 22–26, 2010.
5. Bartusek, K., E. Gescheidtova, and J. Mikulka, "Data processing in studying biological tissues, using MR imaging techniques," *33th International Conference on Telecommunications and Signal Processing*, 171–175, Asszisztenda Szervezo, Budapest, 2010.
6. Mikulka, J., E. Gescheidtova, and K. Bartusek, "Soft-tissues image processing: Comparison of traditional segmentation methods with 2D active contour methods," *Measurement Science Review*, Vol. 12, No. 4, 153–161, 2012.
7. Rupp, R. E., N. A. Ebraheim, and R. J. Coombs, "Magnetic resonance imaging differentiation of compression spine fractures or vertebral lesions caused by osteoporosis or tumore," *Spine*, Vol. 20, 2499–2503, 1995.
8. Marcon, P. and K. Bartusek, "Errors in diffusion coefficients measurement," *PIERS Proceedings*, 1035–1039, Cambridge, USA, Jul. 5–8, 2010.
9. Tsai, J. Z., S. J. Peng, Y. W. Chen, K. W. Wang, H. K. Wu, Y. Y. Lin, Y. Y. Lee, C. J. Chen, H. J. Lin, E. E. Smith, P. S. Yeh, and Y. L. Hsin, "Automatic detection and quantification of acute cerebral infarct by fuzzy clustering and histographic characterization on diffusion weighted MR imaging and apparent diffusion coefficient map," *BioMed Research International*, Vol. 2014, 1–6, Hindawi, 2014.
10. Marcon, P., K. Bartusek, R. Korinek, and Z. Dokoupil, "Correction of artifacts in diffusion-weighted MR images," *34th International Conference on Telecommunications and Signal Processing (TSP)*, 391–397, Budapest, 2011.
11. Wapler, M. C., J. Leupold, I. Dragonu, D. Elverfeld, M. Zaitsev, and U. Wallrabe, "Magnetic properties of materials for MR engineering, micro-MR and beyond," *Journal of Magnetic Resonance*, Vol. 242, 233–242, 2014.
12. McGill, R., J. W. Tukey, and W. A. Larsen, "Variations of boxplots, "*The American Statistician*, Vol. 32, No. 1, 12–16, 1978.
13. Marcon, P., K. Bartusek, E. Gescheidtova, and Z. Dokoupil, "Diffusion MRI: Magnetic field inhomogeneities mitigation," *Measurement Science Review*, Vol. 12, No. 5, 205–212, 2012.
14. Marcon, P., K. Bartusek, M. Burdkova, and Z. Dokoupil, "Magnetic susceptibility measurement using 2D magnetic resonance imaging," *Measurement Science and Technology*, Vol. 22, 2001.